

The Use of Hybrid Bragg Resonators for Generation of Spatial Coherent Radiation by Powerful Relativistic Electron Beams¹

N.S. Ginzburg, V.Yu. Zaslavsky, A.M. Malkin, N.Yu. Peskov, and A.S. Sergeev

*Institute of Applied Physics of RAS, 46, Uljanov str., Nizhny Novgorod, 603950, Russia
Phone: 8(831)416-48-16, 8(831)436-60-86, E-mail: ginzburg@appl.sci-nnov.ru*

Abstract – Periodical Bragg structures can be considered as effective way of controlling the electromagnetic energy fluxes and provision spatial coherence of the radiation in the microwave electron devices with oversized interaction space. A number of problems can be solved using different combination of Bragg structures, including the increase in integral power of coherent radiation and the advance of relativistic electron sources in short millimeter and submillimeter wave bands.

1. Coaxial FEM with two-dimensional distributed feedback

A possibility of drastic increase in radiation power of FEM by extending of interaction space along one of transverse coordinates can be realized on the basis of 2D Bragg structures of both planar and co-axial geometry. Transverse (with respect to translational velocity of electrons) energy fluxes, emerging in these systems, can synchronize the radiation of different parts of sheet and annular electron beams with transverse sizes several orders larger than wavelength [1–3].

In this paper, we consider a model of co-axial FEM with hybrid Bragg resonator which is investigated experimentally in the University of Strathclyde (UK) [3]. 2D Bragg structure represents a section of coaxial waveguide having the length l_1 and the mean radius r_0 with corrugated sidewalls. The corrugation can be presented as a superposition of two helical corrugations (Fig. 1, *a*):

$$a = \frac{a_1}{4} [\cos(\bar{h}_z z - \bar{M}\varphi) + \cos(\bar{h}_z z + \bar{M}\varphi)], \quad (1)$$

where a_1 is the corrugation depth, $\bar{h}_1 = 2\pi/d_1$, d_1 is the corrugation period along z -axis, \bar{M} is the azimuthal number of the corrugation, z and φ are the transverse and azimuthal coordinates, respectively. We assume that the curvature of the waveguide is small, i.e., the waveguide radius is significantly larger than the wavelength λ and the distance between the conductors a_0 . The field in the system under consideration can be presented as a sum of the four coupled

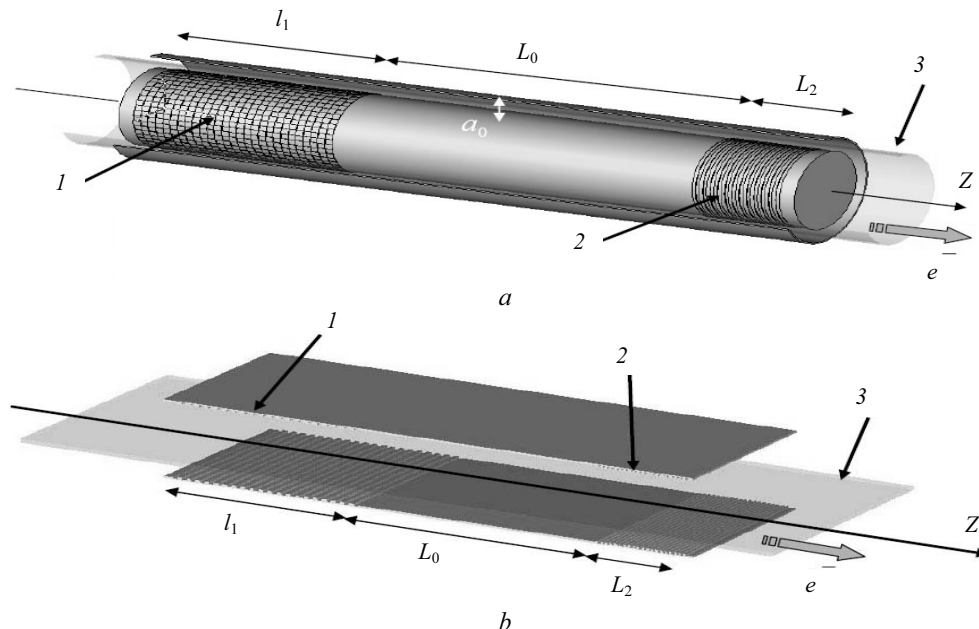


Fig. 1. Schemes of (a) coaxial and (b) planar FEM with hybrid Bragg resonator: 1 – advanced (2D) Bragg reflector; 2 – traditional Bragg reflectors; 3 – electron beam

¹ The work was supported by RFBR (Grants Nos. 06-02-17129-a, 07-02-00617-a, and 08-08-00966-a) and the Dynasty foundation.

waves, two of which (A_{\pm}) propagate in the longitudinal $\pm z$ directions and the other two (B_{\pm}) in the transverse directions:

$$\vec{E} = \text{Re} \left[\begin{pmatrix} A_+ \bar{E}_1^0 e^{ih_1 z} + A_- \bar{E}_1^0 e^{-ih_1 z} + \\ B_+ \bar{E}_2^0 e^{ih_2 x} + B_- \bar{E}_2^0 e^{-ih_2 x} \end{pmatrix} e^{i\bar{\omega} t} \right], \quad (2)$$

where $x = r_0 \varphi$ is the coordinate along the waveguide azimuth, $A_{\pm}(x, z)$ and $B_{\pm}(x, z)$ are the slowly varying amplitudes, $\bar{E}_{1,2}^0(r)$ are the functions specifying the radial structure of the waves, which coincides with the mode structures of regular coaxial waveguide. For the coaxial geometry, the partial waves must obey the cyclicity conditions

$$\begin{aligned} B_{\pm}(x + l_x, z, t) &= B_{\pm}(x, z, t), \\ A_{\pm}(x + l_x, z, t) &= A_{\pm}(x, z, t), \end{aligned} \quad (3)$$

where $l_x = 2\pi r_0$ is the resonator perimeter. These conditions allow the Fourier expansion of the fields:

$$\begin{aligned} A_{\pm}(x, z, t) &= \sum_{m=-\infty}^{\infty} A_{\pm}^m(z, t) e^{2\pi i m x / l_x}, \\ B_{\pm}(x, z, t) &= \sum_{m=-\infty}^{\infty} B_{\pm}^m(z, t) e^{2\pi i m x / l_x}, \end{aligned} \quad (4)$$

and taking each harmonic as a resonator mode with azimuthal index m . Equations for the amplitudes can be presented in the form

$$\begin{aligned} &\left(\frac{\partial}{\partial Z} + \frac{1}{\beta_{gr}} \frac{\partial}{\partial \tau} \right) A_{\pm}^m + \bar{\sigma} A_{\pm}^m + \\ &+ i\hat{\alpha}_1 (B_+^m + B_-^m) = J^m; \\ &\left(-\frac{\partial}{\partial Z} + \frac{1}{\beta_{gr}} \frac{\partial}{\partial \tau} \right) A_{\pm}^m - \bar{\sigma} A_{\pm}^m + \\ &+ i\hat{\alpha}_1 (B_+^m + B_-^m) = 0; \\ &\left(\pm i s m + \frac{1}{\beta_{gr}} \frac{\partial}{\partial \tau} \right) B_{\pm}^m + \frac{iC}{2} \frac{\partial^2 B_{\pm}^m}{\partial Z^2} \pm \\ &\pm \bar{\sigma} B_{\pm}^m + i\hat{\alpha}_1 (A_+^m + A_-^m) = 0. \end{aligned} \quad (5)$$

Here $s = 2\pi/l_x$, $J^m = \frac{1}{2\pi} \int_0^{l_x} J \exp(-ismx) dx$ is the

azimuthal harmonic of RF current: $J = \frac{1}{\pi} \int_0^{2\pi} e^{-i\theta} d\theta_0$,

that can be found by solving the electron motion equations

$$\left(\frac{\partial}{\partial Z} + \beta_{\parallel}^{-1} \frac{\partial}{\partial \tau} \right) \theta = \text{Re} \left\{ \sum_{m=-\infty}^{\infty} A_{\pm}^m(z, t) e^{ismx + i\theta} \right\}, \quad (6)$$

$$\theta \Big|_{z=0} = \theta_s \in [0, 2\pi), \quad \left(\frac{\partial}{\partial Z} + \beta_{\parallel}^{-1} \frac{\partial}{\partial \tau} \right) \theta \Big|_{z=0} = -\Delta,$$

where $\theta = \bar{\omega} t - h z - h_v z$ is the electron phase, $\Delta = (\bar{\omega} - h v_{\parallel} - h_v v_{\parallel}) / \bar{\omega} C$ is the initial detuning of undulator synchronism.

For the partial waves circulating in the azimuthal directions, we apply the radiation boundary conditions on the edges of corrugation

$$B_m \pm \sqrt{\frac{C}{\pi i}} \int_0^{\tau} \frac{e^{(ism - \bar{\sigma})(\tau - \tau')}}{\sqrt{\tau - \tau'}} \frac{\partial B_m(\tau')}{\partial Z} d\tau' \Big|_{z=0, l_x} = 0. \quad (7)$$

In the output traditional Bragg reflector $a = (a_2/2) \cos \bar{h}_2 z$ ($\bar{h}_2 = 2\pi/d_2$, d_2 is the structure period) with the length l_2 (Fig. 1, a) only two partial waves are presented, mutual scattering of which can be described by the equations

$$\begin{aligned} &\frac{\partial A_{m+}}{\partial Z} + \frac{1}{\beta_{gr}} \frac{\partial A_{m+}}{\partial \tau} - i\hat{\alpha}_2 A_{m-} = J; \\ &-\frac{\partial A_{m-}}{\partial Z} + \frac{1}{\beta_{gr}} \frac{\partial A_{m-}}{\partial \tau} - i\hat{\alpha}_2 A_{m+} = 0, \end{aligned} \quad (8)$$

where $\hat{\alpha}_2$ is the coupling coefficient. Amplification of the synchronous wave A_+ in the regular section of resonator is described by the equations (6), (8) where one should put $\hat{\alpha}_2 = 0$. In simulations we assume that the external energy fluxes are absent so the amplitudes of the waves A_{\pm} on the corresponding boundaries turn to zero.

In (5)–(8), we used the following normalized variables and parameters: $Z = zC\bar{\omega}/c$, $X = xC\bar{\omega}/c$, $L_{x,z} = l_{x,z}C\bar{\omega}/c$, C is the amplification parameter $\tau = tC\bar{\omega}$, $(A_{\pm}, B_{\pm}) = (A_{\pm}, B_{\pm})ek\mu/\gamma mc\bar{\omega}C^2$, $k = \beta_{\perp}/\beta_{\parallel}$ is the electron-wave coupling parameter, $\mu \approx \gamma^{-2}$ is the bunching parameter, γ is the relativistic mass factor, $v_{\parallel} = \beta_{\parallel}c$ is the electron translational velocity, $v_{gr} = \beta_{gr}c$ is the wave group velocity; $\bar{\sigma} = \sigma c/\bar{\omega}C$, σ is the Ohmic losses parameter, $\hat{\alpha}_{1,2} = \alpha_{1,2}c/\bar{\omega}C$ is the coupling coefficient.

Simulation carried out at the parameters closed to those realized in the Strathclyde FEM: lengths of the input, output, and regular sections are: $l_1 = 10.4$ cm, $l_2 = 6$ cm, $l_0 = 65$ cm, amplification parameter $C \approx 0.007$, for the resonator made of copper $\sigma \approx 5 \times 10^{-4}$ cm $^{-1}$. Normalized section lengths were $L_1 = 0.6$, $L_0 = 3.7$, and $L_2 = 0.4$, correspondingly, and the coupling coefficient $\hat{\alpha}_1 = 0.5$ and $\hat{\alpha}_2 = 0.35$.

In Fig. 2, zones on the plane: normalized perimeter L_x – the electron synchronism detuning Δ are shown,

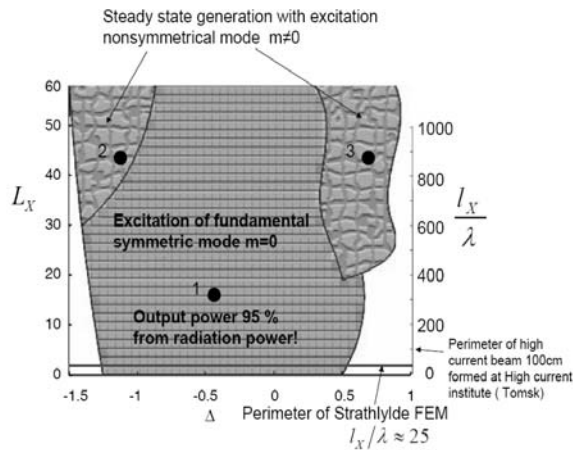


Fig. 2. Zones of stationary generation regimes corresponding to excitation of mode with different number of azimuthal variation m

in which various regimes of oscillation are established. While the perimeter is smaller than the value $L_x \approx 20$ the excitation of a single axial-symmetric mode $m = 0$ with frequency close to the Bragg one in all the variation range of parameter Δ (i.e., in all range of variation of the electron energy) takes place. It is important to note that in the 37 GHz Strathclyde FEM the beam radius 25 cm corresponds to the dimensionless perimeter $L_x = 1.2$. At the present the most powerful annular beam is realized at the Institute of High Current Electronics SB RAS with perimeter about 100 cm [4] which in Ka band corresponds to the normalized perimeter $L_x = 5.5$.

Thus, in the millimeter wave band the use of hybrid Bragg resonators allows realization of single mode single frequency oscillation regime practically for any existing electron beams. Zones of excitation of modes with different azimuthal indices m appear only at the normalized perimeter $L_x > 20$. But even in these zones a steady state regime of generation is also established which corresponds to the synchronization of radiation from the different parts of electron beam. The field distribution of partial waves in the steady-state regime is depicted in Fig. 3, which shows that the main amplification of the signal takes place after the input mirror. As a result, the amplitude of the cutoff mode B_{\pm} excited in the 2D Bragg structure is relatively small. Correspondingly, Ohmic and diffraction losses associated with this mode are also small. Under such conditions up to 95% of energy radiated by the electron beam is extracted with the traveling wave A_{\pm} . Note that in the case when in the simulated experiment a 2D Bragg structure was used as an output mirror, more than half of energy was dissipated in this mirror [3]. Exploiting a hybrid scheme allowed to raise the registered output radiation power several times preserving the estimated electron efficiency about 20%.

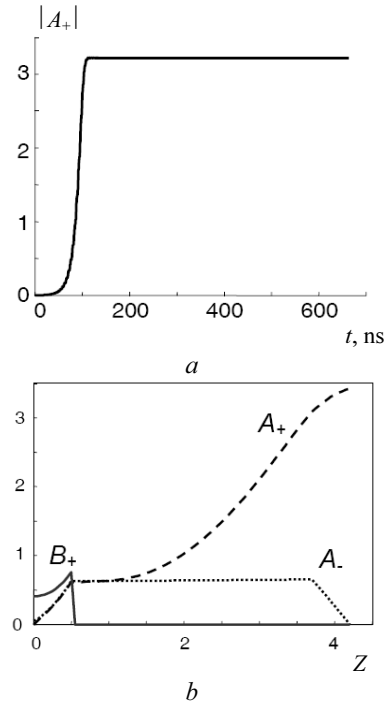


Fig. 3. Modeling of longitudinal modes selection in 37 GHz FEM with hybrid Bragg resonator

2. Short-wave planar FEM with advanced Bragg reflectors

As an effective selective element Bragg structures provide new possibilities for the advance of microwave devices into the short-wave bands. The problem of extending the interaction space along the second (narrow) coordinate y can be solved by using the coupling between the propagating and the quasi cutoff modes in advanced Bragg reflector in which an additional electromagnetic energy fluxes between the plates occurs [5]. Advanced Bragg reflector is formed by the two parallel plates with shallow periodical corrugation of inner walls $b(z) = b_1 \cos(\bar{h}z)$, where $\bar{h} = 2\pi/d_1$, d_1 is the period of the structure (this period is twice large than in traditional reflectors). Under Bragg resonance condition $h \approx \bar{h}$ which is satisfied when the distance between plates $b = nd_{1/2}$. The field can be presented as a sum of the two TEM modes propagating in opposite directions

$$\vec{E}_{\pm} = \text{Re} \left(A_{\pm}(z) \vec{y} e^{i(\omega t \mp hz)} \right) \quad (9a)$$

and cutoff TM_n mode:

$$E = \text{Re} \left(B(z) \vec{y} \sin(\pi nx / b) e^{i\omega t} \right). \quad (9b)$$

The process of reflection via excitation of the cutoff mode can be described by the equations

$$\begin{aligned} \frac{dA_{\pm}}{dZ} \mp i\Omega A_{\pm} &= \pm i\alpha B; \\ \frac{1}{2h} \frac{d^2 B}{dZ^2} + i\sigma B + \Omega B &= \alpha (A_{+} + A_{-}), \end{aligned} \quad (10)$$

with the boundary conditions

$$\frac{dB}{dZ} \mp i\sqrt{2\Omega B} \Big|_{z=0, l_1} = 0, \quad A_+ \Big|_{z=0} = A_0, \quad A_- \Big|_{z=l_1} = 0,$$

where $Z = \bar{h}z$, $\Omega = (\omega - \bar{\omega})/\bar{\omega}$ is the detuning between the Bragg frequency $\bar{\omega} = \bar{h}c$ and that of the incident wave, $\alpha = a_1/2a_0$ is the coupling coefficient.

Neglecting the diffraction for the cutoff mode one can obtain for the reflection coefficient

$$R = \frac{2i(\Omega^2 - K^2) \sin Kl}{(\Omega + K)^2 e^{iKl} - (\Omega - K)^2 e^{-iKl}}, \quad (11)$$

where $K = (\Omega^2 - 2\alpha^2\Omega/(\Omega + i\sigma))^{1/2}$.

Figure 4 shows the frequency dependencies of the reflection coefficient, which demonstrate the selective feature of the advanced Bragg reflector. In difference with the traditional Bragg structures, the decrease of waves coupling coefficient α in this scheme makes the reflection band narrow while the maximum of reflection coefficient does not depend on α being close to unity (nonzero Ohmic losses lead to decrease of R_{\max}).

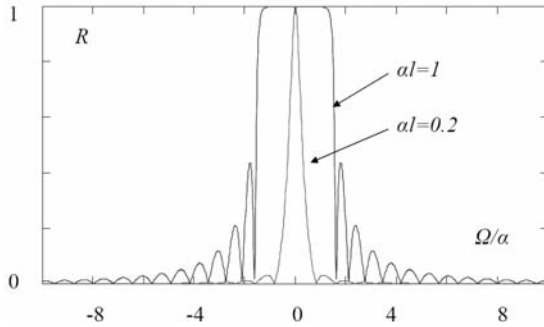


Fig. 4. Reflection coefficient vs frequency in coupled-wave model

Thus, the coupled-wave approach shows that a narrow band reflector effective at large oversize factor can be realized using the coupling between propagating and cutoff modes. This conclusion is confirmed by the results of direct simulation of the advanced Bragg reflector at terahertz frequency band with the use of 3D electromagnetic code. We took the structure period $d = 0.3$ mm, distance between plates $b_0 = 6$ mm, length $l_1 = \dots$. At $n = 20$ expected resonance frequency was $f = 1$ THz. In Fig. 5, the frequency dependence of the reflection and transmission coefficients is shown for the incident TEM mode. One can see that at oversize factor $b_0/\lambda \sim 20$ several reflection bands are presented which correspond to excitation of cutoff modes with different number of field variation

n but reflection near the frequency 1 THz dominated which correspond to the excitation of TM_{20} mode.

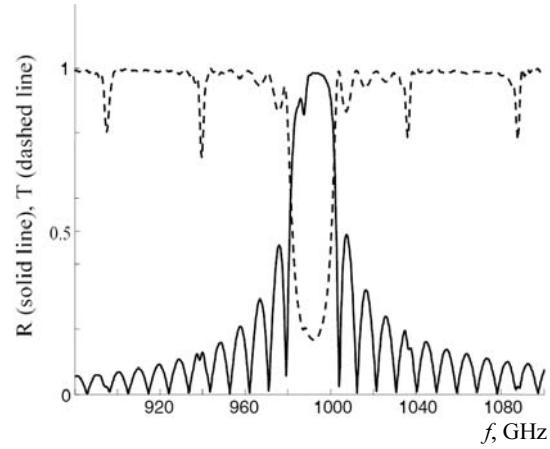


Fig. 5. Reflection and transmission coefficients vs frequency in 3D simulations

As in the previous case it is efficient to use the hybrid resonator for the realization of a planar FEM consisting of an input advanced Bragg reflector and the output traditional Bragg mirror (Fig. 1, *b*). The process of interaction in such device can be described by Eqs. (5)–(8) where $m = 0$ should be put. The simulation of dynamics of novel FEM scheme shows the possibility of effective mode selection over the longitudinal coordinate. The oscillation frequency is close to the cutoff frequency of trapped mode *B* and is not sensitive to the variation of the electron beam parameters. Taking the beam current density 100 A/cm and the electron energy 5 MeV for undulator period 4 cm one can obtain the radiation frequency $f = 1$ THz. For the sheet beam current density 100 A/cm the Pierce parameter is $C \approx 3 \cdot 10^{-4}$. Normalized length $L = 5$ in simulation presented in Fig. 3 corresponds to total length of $l = 80$ cm. Under efficiency 10% power density of THz radiation will be ~ 50 MW/cm. Note that radiation synchronization over *x* coordinate will be provided by cutoff mode *B*.

References

- [1] N.S. Ginzburg et al., Optics Comm. **112**, 151 (1994).
- [2] I.V. Konoplev et. al., Phys. Rev. Lett. **96**, 035002 (2006).
- [3] A.V. Arzhannikov et al., Pis'ma Zh. Eksp. Teor. Fiz. **87**, 715 (2008).
- [4] A.N. Batrikov, Zh. Tekh. Fiz. **58**, 483 (1988).
- [5] N.S. Ginzburg et al., Pis'ma Zh. Tekh. Fiz. **32**, 896 (2006).